QUATERNARY RESEARCH 29, 142–152 (1988)

Origin and Consequences of Cyclic Ice Rafting in the Northeast Atlantic Ocean during the Past 130,000 Years

HARTMUT HEINRICH

Deutsches Hydrographisches Institut, Bernhard-Nocht-Str. 78, D-2000 Hamburg 4, West Germany

Received April 7, 1987

Deep-sea sediment cores recovered from the Northeast Atlantic Ocean were examined in order to elucidate the influence of the Earth's orbital parameters on major ice rafting. Analyses of coarse-grained ice-rafted debris and planktonic foraminifers revealed a strong reaction to the precession signal. Since 130,000 yr B.P., dropstone layers have been deposited each half period of a precessional cycle (11,000 ± 1000 yr). Ice rafting occurs during times of winter minimum/summer maximum insolation and summer minimum/winter maximum insolation. In the first case, high summer insolation forces meltwater discharge from the ice sheets into the polar seas which subsequently enhances formation of sea ice during the winter. In the second case, growth of continental ice enhances iceberg production which also leads to a salinity reduction of surface seawater. Both situations result in a southward penetration of polar water. Thus, the marine record of dropstones documents ice rafting not only during Weichselian stades but also during cold events within interstades. The regularity of ice rafting yields a useful framework to calibrate and elucidate climatic changes, not only in the region of the North Atlantic Ocean but also in remote areas such as the Pacific Ocean and the Antarctic.

INTRODUCTION

The oceanographic and climatic history of the North Atlantic Ocean during the Late Pleistocene has been fairly well known since the publication of the CLIMAP results (Cline and Hays, 1976). Extensive petrographic measurements carried out on hundreds of North Atlantic sediment cores and modern data processing gave quantitative information about the climatic response in this area. Since that time, most efforts have focused on two tasks: to decipher the climatic processes at times of distinct oceanwide environmental changes like glaciation and deglaciation (e.g., Ruddiman *et al.*, 1980; Ruddiman and McIntyre, 1981a) and to resolve the interrelationships among the ocean, the atmosphere, and the continents (e.g., Rind *et al.*, 1986).

The search for the causal mechanisms that initiate climatic processes began much earlier with Milankovitch's (1930) theory of climate control by insolation due to changes in the geometry of the Earth's orbit. His hypothesis was subsequently supported by a number of investigators (e.g, Hays *et al.*, 1976; Berger, 1979), and is now widely accepted. In order to test the orbital influence on climate, cross-spectral analyses between astronomical and sedimentary parameters were carried out (e.g., Herterich and Sarnthein, 1984). Nevertheless, there are many attempts to correlate certain variations of climate with other terrestrial or extraterrestrial mechanisms (e.g., volcanic activity and solar modulation).

The attempts to correlate insolation and Earth's climatic responses as documented in deep-sea sediment from numerous petrographic parameters suffer from the lack of a precise and continuous chronology in the sedimentary successions. Numerical ages are often scarce. Correlations with well-dated sediment cores and interpolation are often affected by various influences during and after deposition, which may have altered the climatic signal (Ruddiman and Glover, 1972; Schiffelbein, 1984). Thus, dating the climate history is primarily a question of sampling optimum sedimentary successions.

The verification of insolation control on

0033-5894/88 $3.00

ice rafting requires sampling in areas with strong climatic contrasts and a set of sensitive indicators. The location should act as a filter; that is, it should be touched only by the stronger pulses of ice rafting. Furthermore, the site should be sensitive not only to cold but also to warm excursions of the climate. These conditions are well fulfilled in the northeastern Atlantic Ocean between latitudes 45° and 50° (Ruddiman and Glover, 1975; Ruddiman and McIntyre, 1976; Ruddiman, 1977).

MATERIAL AND METHODS

In order to avoid impairments from carbonate dissolution and turbidite supply from the distal Maury Channel system (Emery and Uchupi, 1984), sampling had to be carried out on deep-sea hills. The area of investigation (Fig. 1) was carefully mapped with SEA BEAM, 3.5 kHz Subbottom Profiler, and KAE Parasound (Heinrich, 1986a, b). Water depths range from 3900 to 4550 m. There are no obvious differences from those sediments already known in the Northeast Atlantic (Ruddiman and McIntyre, 1976). In general, the sediments on the deep-sea hill (the Dreizack) and in its vicinity consist of intercalated calcareous oozes and poorly calcareous sandy muds. In the Maury turbidity current channel, the pelagic sedimentary sequence is interrupted by thick dark volcaniclastic turbidite layers (Heinrich, 1986b). Submarine landslides, consisting of more than 4 m of semiconsolidated breccias, occur on each side of the Dreizack.

A set of 13 piston cores was collected from the Dreizack and the surrounding deep plain (Fig. 1; Table 1). One Kasten core was taken from an elevated plateau 25 nautical miles northeast of the Dreizack.

The cores were cut and X-ray photographs were made in order to avoid subsampling in burrows of benthic organisms. Subsamples were taken each 3 cm and washed through a 180-μm sieve. Splits of 300 to 600 grains of the coarse fraction were counted for fragments of volcanic glass shards, quartz, volcanic rock, sedimentary rock, and crystalline rock. Fragments >3000 μm in diameter were neglected.

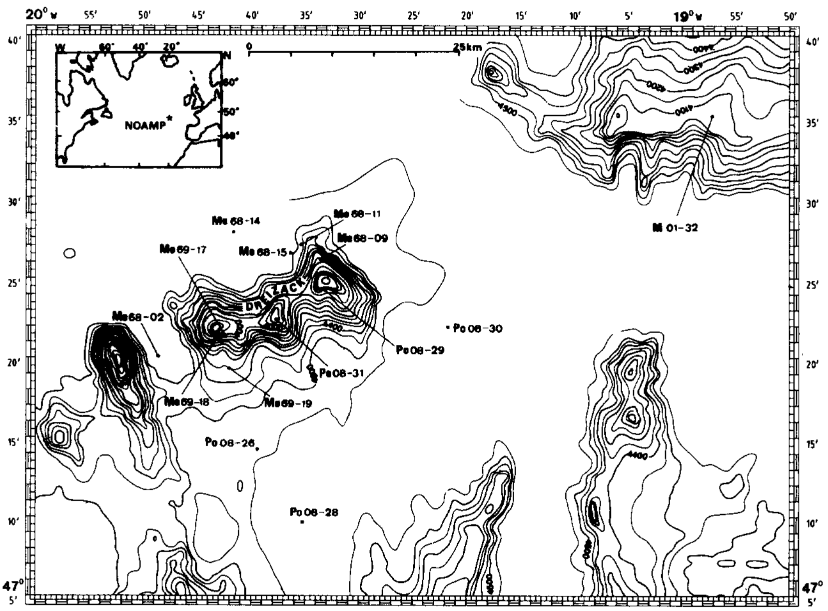

FIG. 1. Bathymetric map (SEA BEAM) of the area around the Dreizack seamount (at 19°40'W, 47°23'N) showing core locations (Table 1). The deep plain is temporarily passed by Maury Channel turbidity currents from west to east. Contour interval = 50 m. The insert shows the position of the NOAMP site in the West-European Basin.

TABLE 1. BOTTOM SAMPLING DATA

Core No.	N Lat.	W Long.	Water depth (m)	Core length (cm)	Corer
Me68-02	47°20.8′	19°48.6′	4510	450	PC6
Me68-09	47°26.3′	19°34.0′	4260	434	PC6
Me68-11	47°26.6′	19°35.5′	4470	549	PC6
Me68-14	47°28.3′	19°43.4′	4545	379	PC6
Me68-15	47°26.8′	19°36.1′	4500	1149	PC12
Me69-17	47°21.4′	19°42.9′	3905	914	PC12
Me69-18	47°20.7′	19°43.3′	4120	1035	PC12
Me69-19	47°19.4′	19°41.3′	4350	1080	PC12
Po08-26	47°14.7′	19°37.1′	4552	1014	PC12
Po08-28	47°10.1′	19°35.8′	4557	2088	PC24
Po08-29	47°24.7′	19°32.9′	3900	968	PC12
Po08-30	47°24.2′	19°22.5′	4550	2238	PC24
Po08-31	47°22.8′	19°38.0′	4030	835	PC12
M01-32	47°34.7′	18°56.0′	4070	360	KC6

Note. Abbreviations: Me, R.V. METEOR (old); Po, R.V. POLARSTERN; M, R.V. METEOR (new); PC, piston corer; KC, Kasten corer.

Dating was by oxygen-isotope stratigraphy based on measurements in core Me69-17. We measured tests of *Pyrgo murrhenia* and *Globigerina bulloides* (Fig. 2). Since benthic foraminifers are very rare in the glacial sediments, a satisfactory deep-water record is not available. An improvement of the oxygen-isotope curve is still in progress. The ages of the boundaries were taken from Herterich and Sarnthein (1984).

In addition, two concentrations of siliceous glass shards were identified as Ash Zone I and Ash Zone II of Bramlette and Bradley (1941). Ruddiman and McIntyre (1984) dated Ash Zone I as 9800 yr B.P. Mangerud *et al.* (1984) correlate this zone with a Norwegian ash layer dated to 10,600 yr B.P. Ash Zone II was estimated to be 65,000 yr old (Ruddiman and Glover, 1972).

RESULTS

Three cores from different physiographic situations in the Dreizack region were taken as representatives (Fig. 1): steep hill crest (Me69-17), flat hill crest or plateau (M01-32), and lower slope (Me69-19).

Stratigraphy

Although most of the Dreizack sediment seemed to be undisturbed in the radiographs (except the breccias), nannofossil and paleomagnetic analyses revealed numerous discordances. Because all hiatuses were older than the oxygen-isotope stage 6/5 boundary, investigations of ice rafting

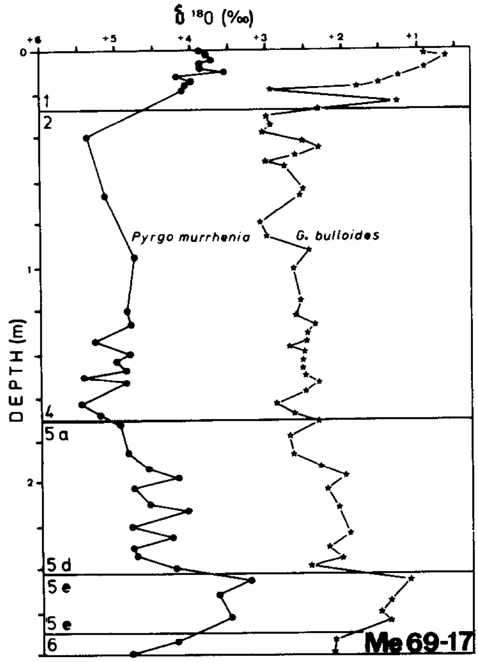

FIG. 2. Oxygen-isotope record of core Me69-17. Measurements were carried out on the benthic species *Pyrgo murrhenia* and the planktic *Globigerina bulloides*. No benthic foraminifers were found within the dropstone layers. The ages of the stage bounderies originate from Herterich and Sarnthein (1984).

were restricted to the last 140,000 yr. The oxygen-isotope record of the species *P. murrhenia* clearly revealed stage boundaries 2/1, 5a/4, 5e/5d, and 6/5 (Fig. 2). Stage 5a/4 boundary has been assigned to the *G. inflata* maximum beneath IRD peak 6 (SST maximum according to Ruddiman *et al.*, 1980). The record of stages 2 to 4 was insufficient due to the very sparse occurrence of benthic tests. Ash layers I and II were obvious in all cores.

Ice-Rafted Debris (IRD)

The majority of the ice-rafted particles in the fraction 180 to 3000 μm consists of transparent angular quartz grains. Few of these grains are well-rounded and scratched. Fragments of plutonic and volcanic rocks are rare. Fragments of sedimentary rocks occur only in the fraction >3000 μm.

The record of ice-rafted debris is nearly uniform in all cores. From the top down to the isotope stage 5/4 boundary all cores yield six distinct peaks (Figs. 3–5). Undisturbed core tops and additional analyses of precise surface samples of multicorers reveal a seventh enrichment of quartz, on the order of 5 to 10%, in the surface sediment. This coincides with the occurrence of large faceted pebbles on the sediment surface observed in box cores and bottom photographs.

In oxygen-isotope stage 5, the number of clearly visible peaks is reduced to one in the upper part of this stage, a slight enrichment at the 5e/5d boundary, and a large one at the 6/5 boundary. Although the cores originate from different physiographic positions, the shape of the IRD peaks is rather regular. The uppermost four peaks are always very large, whereas the fifth peak is a narrow one. The peak between Ash Layer II and the isotope stage 5/4 boundary has a very broad base. The peaks of stage 5 are generally weaker than the younger ones. While

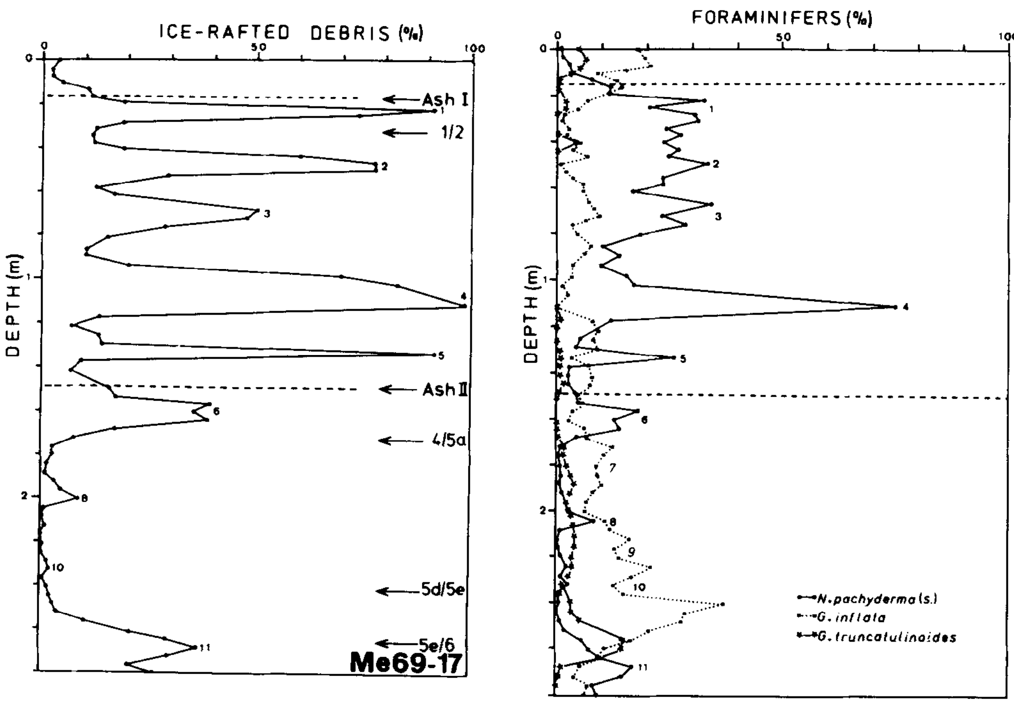

FIG. 3. Core record of Me69-17 from the western peak of the Dreizack. The amount of ice-rafted debris is given as part of the total split (IRD + forams). The amount of one species is given as part of the sum of planktonic forams in a split. The right side of the IRD record shows the stratigraphic markers (Ash I and II, oxygen-isotope stage boundaries).

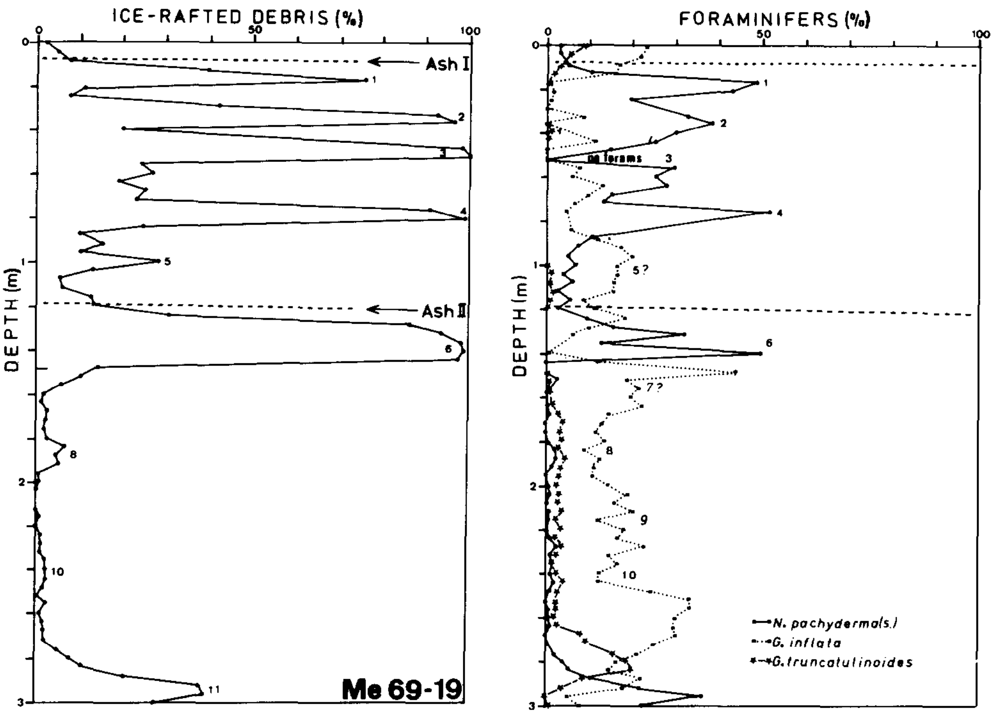

FIG. 4. Core record of Me69-19 (from the southwestern foot of the Dreizack). See Figure 2 for modes of calculation.

the peak in the upper part of stage 5 is always easy to recognize, there is only a very weak enrichment of quartz grains above the 5e/5d boundary.

Foraminifera

Seven species of planktic foraminifera were used to characterize surface cold water: *N. pachyderma* (s.) and *G. bulloides;* surface temperate water: *G. inflata;* and surface warm water: *G. truncatulinoides, G. scitula, G. ruber* (w), and *G. hirsuta.* The results based on these species are given in Figures 3–5. The foraminiferal record does not present such a clear picture as the IRD. In general, the most abundant species in the grain-size fraction >180 μm are *G. bulloides, N. pachyderma* (d.), and *G. inflata.*

Although these curves are rather sawtoothed in shape, there are clear corresponding features in all cores. *N. pachyderma* (s.) matches nearly perfectly with the IRD record. Where the amount of IRD is high, the polar representative is also abundant. *G. inflata* culminates between the *N. pachyderma* (s.) peaks. The highest abundances occur shortly before substage 5e/5d boundary. Subtropical to tropical species, especially *G. truncatulinoides,* are common in the Holocene and throughout isotope stage 5. They culminate in the mid-Holocene and in early substage 5e. The precise surface samples reveal a strong decrease since the mid-Holocene maximum. It is worthy of note that subtropical species occurred in the time shortly after the deposition of Ash layer II.

The sediment accumulation rates of the cores (Fig. 6) have been rather constant since the isotope stage 6/5 boundary: 2 cm/1000 yr in Me69-17 and in Me69-19 and 3 cm/1000 yr in M01-32, although sedimentation varied repeatedly from calcareous ooze to clayey quartz sand.

DISCUSSION

The positions of the IRD peak maxima in the time/depth graphs show that the respective peaks correlate fairly closely between the cores (Fig. 6). Since all cores were recovered from the same area of the northeast Atlantic Ocean, each set of peaks probably has the same age. Thus, the age differences between the respective peaks observed originate from local variations in accumulation rate and from uncertainties in the exact depths of the IRD maxima in the cores.

The search for true ages of the IRD layers, and for the trigger of the respective ice rafting, leads to a comparison of the estimated ages deduced from the accumulation rate and of the variations of the solar radiation received on Earth. As can be seen in Figure 7, phases of intense ice rafting match perfectly with the precessional influence on Northern Hemisphere insolation. At times of a precessional angle of $\Pi = 90°$, the Northern Hemisphere receives a reduced insolation during summer and a slightly increased insolation during winter. At times of a precessional angle of $\Pi = 270°$, the summer insolation is elevated and the winter insolation is reduced (Vernekar, 1972; Berger, 1978). Thus, there are two opportunities of enhanced ice rafting in the northeast Atlantic Ocean during one cycle of the Earth's precession (i.e., every 11,000 ± 1000 yr).

Two insolation minima are not represented by dropstone layers. Their estimated positions in the core records are marked by italic numbers 7 and 9 in Figures 3–5. These two peaks belong to the precessional angle $\Pi = 270$ at 83,000 and 103,000 yr B.P. Assuming that the mean temperature was relatively warm during those times (as indicated by the occurrence of *G. truncatulinoides*), it seems that ice rafting was restricted to the polar seas. Nevertheless, the diminished insolation might have led to a cooling of Northeast Atlantic surface waters, which would have caused the retreat of temperate planktonic species in the foraminiferal core records. The decrease of *G.*

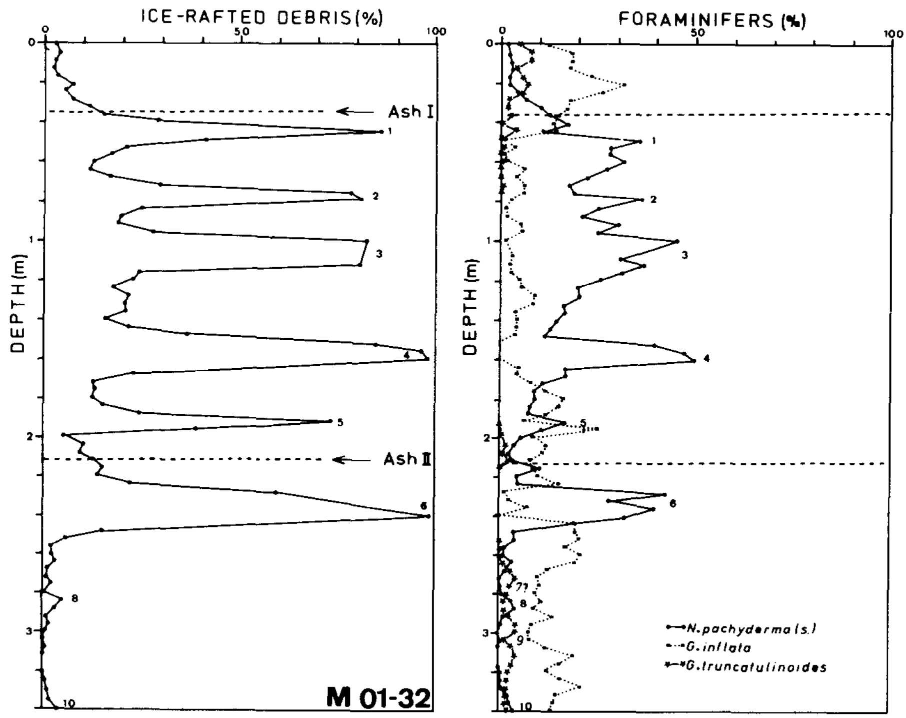

FIG. 5. Core record of M01-32 (from the elevated plateau northeast of the Maury turbidite channel). See Figure 2 for modes of calculation.

inflata, which is best illustrated in core Me69-17, could be related to this cooling.

Although ice rafting is obviously linked to the precession, it is difficult to estimate the exact dates and duration of these phases. If the modes of "ice-sheet decay" and "ice-sheet growth" are correct (Ruddiman and McIntyre, 1981b), enhanced summer insolation initiates the decay of the ice sheets (at times of $\Pi = 270$). Large meltwater supply to the ocean reduces the salinity of the surface water and favors freezing during the long, cold winters. Thus, ice which floats across the Northeast Atlantic during times of ice-sheet decay is mainly sea ice containing little continental debris, with a subordinate influx of material transported by icebergs. This is emphasized by the reduced width of the peaks with odd numbers (Figs. 3–5). It seems reasonable to place these peaks very close to the times of the winter insolation minima due to a strong recessional response of the ice sheets upon the controlling reduction of insolation (Hyde and Peltier, 1987).

In contrast, the temporal linking of ice rafting and insolation at times of a precessional angle of $\Pi = 90°$ is more difficult. There has to be a certain delay between ice-sheet construction and Northeast Atlantic ice rafting because both can hardly occur at the same time.

Ruddimen *et al.* (1980) infer that ice-sheet construction is initiated, among other reasons, by an intensified supply of warm surface water into the high-latitude North Atlantic. During these times, with a strong North Atlantic Drift, ice rafting across the Northeast Atlantic Ocean seems rather improbable. In this area, ice rafting may occur when enhanced discharges of cold, less-saline surface water from the northern

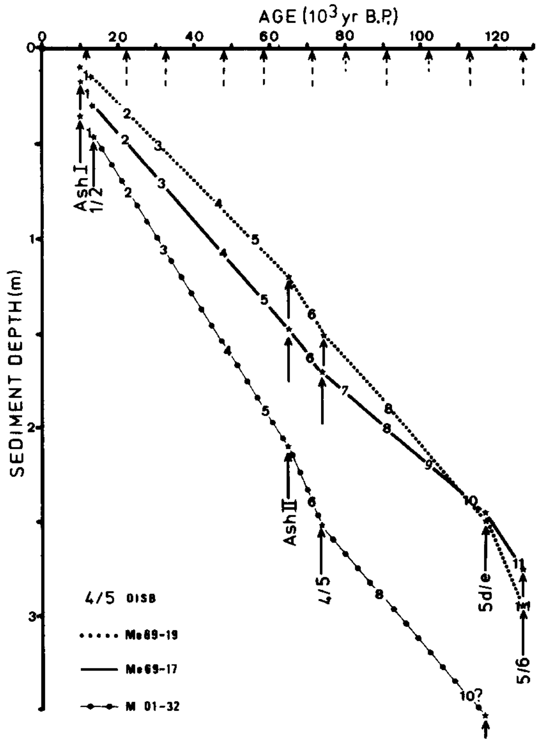

FIG. 6. Age/depth correlation of the dropstone peaks. The apparent ages of the peaks are obtained by interpolation between the stratigraphic markers indicated by arrows. OISB, oxygen-isotope stage boundary.

oceans bend the North Atlantic Drift to more southerly directions. Indeed, in the stage 5/4 transition, the warm North Atlantic Drift water rich in *G. inflata* was replaced by cold Arctic water which brought ice-rafted detritus and polar foraminifers down to lower latitudes (Ruddiman *et al.*, 1980).

A possible mechanism which might have initiated increased formation of cold surface water results from decreasing stabilities of continental ice sheets during enhanced ice accumulation (Reeh, 1985). This leads to a faster lateral progression of the continental ice sheets and, subsequently, to a greater discharge of ice into the ocean. The fresh water supply from large numbers of melting icebergs reduces the salinity of the oceanic surface water. Therefore, the oxygen-isotope ratios of *G. bulloides* tests became low in the youngest Weichselian dropstone layers when ice rafting reached its greatest extent (Fig. 2).

If the magnitude of ice-sheet growth is primarily a function of interacting orbital parameters (Saltzman *et al.*, 1984), inception and duration of a single ice-rafting phase should be variable. Nevertheless, the mean ages of the dropstone layers derived from accumulation rates in relation to orbital data reveal a considerable coincidence of insolation minimum and maximum ice rafting in the northeastern Atlantic Ocean (Fig. 7).

SUMMARY AND CONCLUSIONS

Since the Eemian interglaciation, major Northeast Atlantic ice rafting has been primarily controlled by the precession of the Earth's axis. It is linked to (a) summer and (b) winter insolation minima which occur two times during one precessional cycle (at precession angles (a) $\Pi = 90°$ and (b) $\Pi = 270°$). Thus, the mean period of enhanced ice rafting is about 11,000 ± 1000 yr. Inception, length, and intensity of an ice-rafting phase depend on the interactions with such other basic parameters as obliquity and eccentricity. The dropstone record indicates

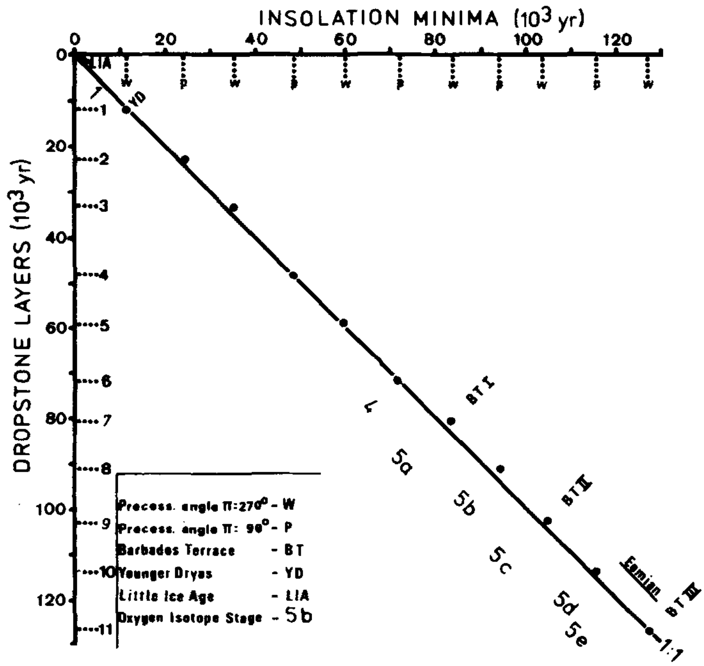

FIG. 7. Relationship of dropstone ages (from Fig. 6) and times of insolation minima (from Vernekar, 1972).

ice rafting not only during stadial intervals but also more or less in the middle of interstades.

At times when the precessional angle $\Pi = 270°$, Northern Hemisphere ice rafting is probably coupled with enhanced formation of winter sea ice which benefits from a forced meltwater supply into the ocean due to high summer insolation. At times when the precessional angle $\Pi = 90°$, ice rafting across the northeastern Atlantic Ocean seems to be a consequence of increased ice discharge which results from continental ice-sheet growth due to reduced summer insolation in the higher latitudes. In both cases, the crucial point for major ice rafting is the intensified formation of cold, less-saline surface water which favors the transport of ice down to the latitude of the Iberian Peninsula (McIntyre *et al.*, 1972). This occurs essentially during times when $\Pi = 90°$. The southward penetration of polar water then keeps warm North Atlantic Drift water away from the northern part of the ocean and reduces the transport of moisture to the ice sheets.

The systematic changes of major Northern Hemisphere ice rafting since the Eemian correspond with many other climate records from different fields and regions. As illustrated by the New Guinea sea-level curve (Bloom *et al.*, 1974; Chappell and Veeh, 1978), relevant drops correlate with the dropstone layers of the precessional angle $\Pi = 90°$. The winter insolation minimum (precessional angle $\Pi = 270°$) causes obviously minor sea-level drops because these phases of enhanced ice rafting coincide precisely with dated relative high sea stands which are, for example, indicated by coral terraces on Barbados (Broecker *et al.*, 1968).

Furthermore, the improved dropstone stratigraphy explains certain climatic events better than before. Two intervals of enhanced ^{10}Be deposition in Antarctic ice at 60,000 and 35,000 yr B.P., which were interpreted as changes in solar modulation (Raisbeck *et al.*, 1987), match perfectly with climatic situations during $\Pi = 270°$. It seems reasonable to correlate the cold Younger Dryas oscillation with the precessional winter insolation minimum (Fig. 7). Warm climatic events (61,000 yr B.P.) recorded in the Spitsbergen area off northern Norway (Gard, 1986) can be attributed to the precessional phase with increased summer insolation. Mangerud *et al.* (1979) report interstadial ice-sheet retreats in Scandinavia between 38,000 and 28,00 yr B.P. which correlate well with the period of enhanced summer insolation at that time.

As can be seen in Figure 7, the distance from the last major IRD deposition to the present occupies one interval between two phases of ice rafting. Indeed, the precessional angle $\Pi = 90°$ was reached in the middle of the 14th century (Bouvier, 1983). Therefore, it is more likely that the Little Ice Age (1350–1900 A.D.) is a very cool part of the whole phase of reduced summer insolation than a consequence of enhanced volcanic activity (Hammer *et al.*, 1980; Dansgaard, 1984; Porter, 1986).

ACKNOWLEDGMENTS

I thank the Masters and crews of both RVs *Meteor* and RV *Polarstern* for their help. D. Meischner (Göttingen) and C. Hemleben (Tübingen) supported the investigation with fruitful discussions. H. Oberhänsli (Zürich) carried out stable oxygen- and carbon-isotope analyses. R. Jantschik and R. Lohoff (Göttingen) carried out sampling and core descriptions. The NOAMP study is funded by the Bundesminister für Forschung u. Technologie, No. KWA 5310.

REFERENCES

Berger, A. L. (1978). Long-term variations of caloric insolation resulting from the Earth's orbital elements. *Quaternary Research* **9**, 139–167.

Berger, A. (1979). Spectrum of climatic variations and their causal mechanisms. *Geophysical Surveys* **3**, 351–402.

Bloom, A. L., Broecker, W. S., Chappell, J. A. M., Matthews, R. K., and Mesolella, K. J. (1974). Quaternary sea level fluctuations on a tectonic coast: New 230Th/234U dates from the Huon Peninsula, New Guinea. *Quaternary Research* **4**, 185–205.

Bouvier, J.-M. (1983). An astronomical approach to human prehistoric ecology: Quantitative insolation at Late Würm in south-west France. Actes Coll. AGSO Bordeaux, Mai 1983, *Bulletin de l'Institut de Geologie du Bassin d'Aquitaine*, **34**, and *CNRS Cahiers du Quaternaire*, Special edition, pp. 27–35.

Bramlette, M. N., and Bradley, W. H. (1941). "Geology and Biology of North Atlantic Deep-Sea Cores between Newfoundland and Ireland: I. Lithology and Geologic Interpretation." U.S. Geological Survey Professional Paper, 196-A, pp. 1–34.

Broecker, W. S., Thurber, D. L., Goddard, J., Ku, T.-L., Matthews, R. K., and Mesolella, K. J. (1968). Milankovitch hypothesis supported by precise dating of coral reefs and deep-sea sediments. *Science* **159**, 297–300.

Chappell, J., and Veeh, H. H. (1978). 230Th/234U age support of an interstadial sea level of −40 m at 30,000 yr B.P. *Nature (London)* **276**, 602–603.

Cline, R. M., and Hays, J. D., Eds. (1976). Investigation of Late Quaternary paleoceanography and paleoclimatology. *Geological Society of America Memoir* **145**.

Dansgaard, W. (1984). The future degree of glaciation. *In* "The Climate of Europe: Past, Present and Future" (H. Flohn and R. Frantechi, Eds.), pp. 225–248. Reidel, Dordrecht.

Emery, K. D., and Uchupi, E. (1984). "The Geology of the Atlantic Ocean." Springer-Verlag, New York.

Gard, G. (1986). Calcareous nannofossil biostratigraphy of Late Quaternary Arctic sediments. *Boreas* 15(3), 217–230.

Hammer, C. U., Clausen, H. B., and Dansgaard, W. (1980). Greenland ice sheet evidence of post-glacial volcanism and its climatic impact. *Nature (London)* **288**, 230–235.

Hays, J. D., Imbrie, J., and Shackleton, N. J. (1976). Variations in the earth's orbit: Pacemaker of the Ice Ages. *Science* **194**, 1121–1132.

Heinrich, H. (1986a). Bathymetrie und Geomorphologie des NOAMP-Gebietes, Westeuropäisches Becken (17W bis 22W, 46N bis 49N). *Deutsche Hydrographische Zeitschrift* **39**, 183–196.

Heinrich, H. (1986b). A comparison of conventional ship-installed 3.5 kHz Sub Bottom Profiler and the new KAE "Parasound" illustrated by an acoustic mapping of a deep-sea meander. *Deutsche Hydrographische Zeitschrift* **39**, 255–262.

Herterich, K., and Sarnthein, M. (1984). Brunhes time scale: Tuning by rates of calcium-carbonate dissolution and cross spectral analyses with solar insolation. *In* "Milankovitch and Climate" (A. Berger, *et al.*, Eds.), Part 1. Vol. 126, pp. 447–466. NATO ASI Series C, Reidel, Dordrecht.

Hyde, W. T., and Peltier, W. R. (1987). Sensitivity experiments with a model of the Ice Age cycle: The response to Milankovitch Forcing. *Journal of the Atmospheric Sciences* **44**(10), 1351–1374.

Mangerud, J., Larsen, E., Longva, O., and Sonstegaard, E. (1979). Glacial history of Western Norway 15,000–10,000 B.P. *Boreas* **8**, 179–187.

Mangerud, J., Lie, S. E., Furnes, H., Kristiansen, I. L., and Lomo, L. (1984). A Younger Dryas ash bed in Western Norway, and its possible correlation with tephra in cores from the Norwegian Sea and the North Atlantic. *Quaternary Research* **21**, 85–104.

McIntyre, A., Ruddiman, W. F., and Jantzen, R. (1972). Southward penetration of the North Atlantic Polar Front: Faunal and floral evidence of large-scale surface water mass movements over the last 225,000 years. *Deep-Sea Research* **19**, 61–77.

Milankovitch, M. (1930). Mathematische Klimalehre und astronomische Theorie der Klimaschwankungen. *In* "Handbuch der Klimatologie" (W. Köppen and R. Geiger, Eds.), I(A). Bornträger, Berlin.

Porter, S. C. (1986). Pattern and forcing of Northern Hemisphere glacier variations during the last millennium. *Quaternary Research* **26**, 27–48.

Raisbeck, G. M., Yiou, F., Bourles, D., Lorius, C., Jouzel, J., and Barkov, N. I. (1987). Evidence for two intervals of enhanced 10-Be deposition in Antarctic ice during the last glacial period. *Nature (London)* **326**, 273–277.

Reeh, N. (1985). Was the Greenland ice sheet thinner in the late Wisconsin than now? *Nature (London)* **317**, 797–799.

Rind, D., Peteet, D., Broecker, W. S., McIntyre, A., and Ruddiman, W. F. (1986). The impact of cold North Atlantic sea surface temperatures on climate: Implications for the Younger Dryas cooling (11–10 k). *Climate Dynamics* **1**(1), 3–33.

Ruddiman, W. F. (1977). Late Quaternary deposition of ice-rafted sand in the subpolar North Atlantic (lat 40 to 65). *Geological Society of America Bulletin* **88**, 1813–1827.

Ruddiman, W. F., and Glover, L. K. (1972). Vertical mixing of ice-rafted volcanic ash in North Atlantic sediments. *Geological Society of America Bulletin* **83**(9), 2817–2835.

Ruddiman, W. F., and Glover, L. K. (1975). Subpolar North Atlantic circulation at 9300 yr BP: Faunal evidence. *Quaternary Research* **5**, 361–389.

Ruddiman, W. F., and McIntyre, A. (1976). Northeast Atlantic paleoclimatic changes over the past 600,000 years. *Geological Society of America Memoir* **145**, 111–146.

Ruddiman, W. F., and McIntyre, A. (1981a). The North Atlantic during the last deglaciation. *Palaeogeography, Paleoclimatology, Palaeoecology* **35**, 145–214.

Ruddiman, W. F., and McIntyre, A. (1981b). Oceanic mechanisms for amplification of the 23,000-year ice-volume cycle. *Science* **212**, 617–627.

Ruddiman, W. F., and McIntyre, A. (1984). Ice-age thermal response and climatic role of the surface

Atlantic Ocean, 40N° to 63°N. *Geological Society of America Bulletin* **95**, 381–396.

Ruddiman, W. F., McIntyre, A., Niebler-Hunt, V., and Durazzi, J. T. (1980). Oceanic evidence for the mechanism of rapid northern hemisphere glaciation. *Quaternary Research* **13**, 33–64.

Saltzman, B., Hansen, A. R., and Maasch, K. A. (1984). The late Quaternary glaciations as the response of a three-component feedback system to Earth-orbital forcing. *Journal of the Atmospheric Sciences* **41**, 3380–3389.

Schiffelbein, P. (1984). Effect of benthic mixing on the information content of deep-sea stratigraphical signals. *Nature (London)* **311**, 651–653.

Vernekar, A. D. (1972). Long-period global variations of incoming solar radiation. Meteorological Monographs **12**, 1–21.